

ANALYSIS OF THE IN VIVO FUNCTIONS OF Mrp3

MARTIN G. BELINSKY, PAUL A DAWSON, IRINA SHCHAVELEVA, LISA J. BAIN,
RENXUE WANG, VICTOR LING, ZHE-SHENG CHEN, ALEX GRINBERG, HEINER
WESTPHAL, ANDRES KLEIN-SZANTO, ANTHONY LERRO, and GARY D. KRUEH

From the Medical Science (M.G.B, I.S., Z-S. C., A.K-S. and G.D.K) and Basic Science
Divisions (A.L.), Fox Chase Cancer Center, Philadelphia PA 19111, Department of Internal
Medicine, Wake Forest University School of Medicine, Winston-Salem, NC 27157 (P.A.D.),
Department of Biological Sciences, University of Texas at El Paso, TX 79968 (L.J.B), British
Columbia Cancer Agency, Vancouver, BC, Canada V5Z 1L3 (R.W. and V.L.), National
Institute of Child Health and Human Development, National Institutes of Health, Bethesda, MD
20892 (A.G. and H.W.)

Running Title: In Vivo Function of Mrp3

Address correspondence to: Gary D. Kruh, Medical Science Division, Fox Chase Cancer Center, 333 Cottman Avenue, Philadelphia, PA 19111, Tel. 215-728-5317; Fax. 215-728-3603; E-mail: Gary.Kruh@fccc.edu

Text pages: 14 (introduction through end of discussion)

Tables: 2

Abstract, words: 253

Introduction, words: 777

Discussion, words: 1158

The abbreviations used are: MRP, multidrug resistance protein; *Abcc3* is the gene symbol for *Mrp3*; ASBT, apical sodium-dependent bile acid transporter; Bsep, bile salt export pump (Spgp is an alternative name).

ABSTRACT

MRP3 is an ABC transporter that is able to confer resistance to anticancer agents such as etoposide and to transport lipophilic anions such as bile acids and glucuronides. These capabilities, along with the induction of MRP3 protein on hepatocyte sinusoidal membranes in cholestasis, and expression of MRP3 in enterocytes, have led to the hypotheses that MRP3 may function in the body to protect normal tissues from etoposide, to protect cholestatic hepatocytes from endobiotics and to facilitate bile acid reclamation from the gut. To elucidate the role of Mrp3 in these processes the *Mrp3* gene (*Abcc3*) was disrupted by homologous recombination. Homozygous null animals were healthy and physically indistinguishable from wild-type mice. *Mrp3*^{-/-} mice did not exhibit enhanced lethality to etoposide phosphate, although analysis of transfected HEK293 cells indicated that the potency of murine Mrp3 towards etoposide (~2.0-2.5-fold) is comparable to that of human MRP3. Following induction of cholestasis by bile duct ligation, *Mrp3*^{-/-} mice had 1.5-fold higher levels of liver bile acids and 3.1-fold lower levels of serum bilirubin glucuronide compared to ligated wild-type mice, whereas significant differences were not observed between the respective sham-operated mice. Bile acid excretion, pool size and fractional turnover rates were similar in *Mrp3*^{-/-} and wild-type mice. We conclude that Mrp3 functions as an alternative route for the export of bile acids and glucuronides from cholestatic hepatocytes, that the pump does not play a major role in the enterohepatic circulation of bile acids, and that the lack of chemosensitivity is likely attributable to functional redundancy with other pumps.

MRP3 belongs to a group of nine related ATP binding cassette transporters that constitute the MRP family. Members of this family function as efflux pumps for lipophilic anions and hydrophobic compounds (Kruh and Belinsky, 2003). The *in vivo* functions of the first two members of this family have been investigated in gene-disrupted mice in the case of Mrp1, and hereditarily deficient rats (EHBR and TR⁻ rats) and humans (Dubin-Johnson syndrome) in the case of Mrp2. These studies indicate that MRP1 functions as an *in vivo* resistance factor for anticancer agents and in inflammatory responses mediated by leukotriene C₄ (Johnson et al., 2001; Lorico et al., 1997; Schultz et al., 2001; Wijnholds et al., 1997) and that MRP2 is involved in the hepatobiliary elimination of endogenous compounds such as bilirubin glucuronide and in the hepatobiliary and renal elimination of xenobiotics (Gerk and Vore, 2002). In contrast to MRP1 and MRP2, the *in vivo* functions of MRP3 have not been established. However, studies in our laboratory and others on the pump's substrate selectivity, resistance capabilities and tissue expression pattern have allowed speculation as to its functions in the body. In cellular models ectopic expression of human MRP3 is able to confer resistance to etoposide and methotrexate, results which are consistent with the hypothesis that the pump is *in vivo* resistance factor that protects normal tissues from chemotherapeutic agents (Kool et al., 1999; Zeng et al., 1999; Zeng et al., 2001). The substrate selectivity of human and rat Mrp3 is similar to that of MRP1 and MRP2 with respect to the ability to transport glucuronate and glutathione conjugates, but in contrast to the latter two pumps monoanionic bile acids are also good substrates of MRP3 (Hirohashi et al., 1999; Hirohashi et al., 2000; Zeng et al., 2000). MRP3 assumes basolateral subcellular localization in polarized cells, and is expressed in a variety of tissues including kidney, gut and pancreas (Belinsky et al., 1998; Rost et al., 2002; Scheffer et al., 2002). Notably, its expression is dramatically increased at the hepatocyte sinusoidal membrane in cholestatic conditions (Donner and Keppler, 2001; Soroka et al., 2001, and references therein). The ability of MRP3 to transport bile acids, glucuronides and other compounds that are normally transported across the canalicular membrane by MRP2 and the bile salt export pump, in combination with induction of MRP3 in cholestasis, have led to the hypothesis that MRP3 protects hepatocytes by functioning as an alternate route of elimination when the canalicular route of detoxification is impaired. This notion is also supported by

studies showing that Mrp3 is induced by bile acids, and that Mrp3 expression is linked to signal transduction and transcriptional pathways that govern bile acid homeostatic mechanisms (Bohan et al., 2003; Inokuchi et al., 2001; Zollner et al., 2003). While mice deficient in some of these transcriptional pathways are more susceptible to liver damage when made cholestatic, the extent to which attenuation of MRP3 induction may contribute to this process, as opposed to impairments in the pleiotropic mechanisms of bile acid homeostasis that are regulated by these transcriptional pathways, is unknown (Bohan et al., 2003; Zhang et al., 2004). MRP3 has also been implicated in the enterohepatic circulation of bile acids. Bile acids are transported from the intestinal lumen across the enterocyte brush border membrane by the well-characterized ileal apical bile acid transporter (ASBT). However, the mechanisms responsible for bile acid transport across the enterocyte basolateral membrane have not been fully identified. By virtue of its basolateral membrane expression in enterocytes and its bile acid transport properties, it has been proposed that MRP3 functions as the intestinal basolateral bile acid transporter that moves bile acids from the enterocyte into the portal circulation.

Here, *Mrp3*^{-/-} mice were generated and analyzed to investigate the *in vivo* functions of Mrp3. *Mrp3*^{-/-} mice did not exhibit increased sensitivity to etoposide phosphate, although transfection experiments showed that expression of the murine protein in HEK293 cells is capable of conferring resistance to this agent. Whereas *Mrp3* null mice are healthy and have normal bile flow, these animals accumulate increased levels of hepatic bile acids and have reduced serum levels of bilirubin glucuronide following bile duct ligation. Measurements of overall bile acid metabolism, including fecal bile acid excretion, bile acid pool size and bile acid fractional turnover rate were similar in *Mrp3*^{-/-} and wild-type mice. Based upon these findings it is concluded that Mrp3 functions as an alternative route for the export of bile acids and glucuronides in cholestatic hepatocytes, that the pump does not play a major role in the enterohepatic circulation of bile acids, and that the lack of chemosensitivity in *Mrp3*^{-/-} mice may be attributable to functional redundancy with other efflux pumps.

Materials and Methods

Targeted disruption of the *Mrp3* gene and generation of *Mrp3*^{-/-} mice. A 1 kb fragment containing the 5' end of the *Mrp3* coding sequence was used to screen a mouse strain 129-derived λ phage genomic library and a ~9 kb *Mrp3* clone was isolated. The *Mrp3* genomic clone was sequenced using an ABI 377 DNA sequencer and encompassed exons 2 to 11 of the *Mrp3* gene, corresponding to nucleotides 100-1482 of the coding sequence. The left and right arms of a targeting vector were generated by polymerase chain reaction and inserted, respectively, to the 5' and 3' of the *pgk-neo* cassette in the PNT plasmid. The vector was designed to delete exons 6-8, encoding nucleotides 613-996 of the coding sequence, and to introduce a frame-shift into the transcribed RNA sequence. The nucleotide sequence of the cloned arms was confirmed, and the resulting ~ 12 kb vector was digested with *NotI*. The linearized DNA was electroporated into strain 129-derived R1 embryonic stem cells. Individual colonies isolated following positive/negative selection with G418 and gancyclovir were screened by Southern blot analysis using 5' and 3' probes and genomic DNA digested with *XhoI/XmnI*. In addition, the absence of randomly integrated vector sequences was confirmed by Southern blot analysis using a *neo* probe. Two correctly targeted ES cell lines were injected into C57/BL6 blastocysts, and the blastocysts were implanted in pseudopregnant females. Male chimeric progeny were crossed with female C57BL/6J (in-house bred) mice. Germ-line transmission of the targeted allele was confirmed by Southern blot analysis and subsequent genotyping was accomplished by PCR analysis of tail DNA. The latter reaction was carried out in a single tube using three primers: 5'-gttctgtgccctcatctgtcc-3', 5'-gggagggggcaagtcaggcc-3', and 5'-aattgacctgcaggggcctcg-3'. The former two primers generate a 790 bp wild-type product, and the latter two generate a 330 bp product from the targeted allele. The *Mrp3* null allele was subsequently backcrossed for 8 generations into the C57BL/6J background. As indicated below, *Mrp3* null mice in the mixed C57BL/6J x 129 background and the C57BL/6J background were used for these studies.

Isolation of *Mrp3* cDNA, expression vector construction and transfection. A PCR product corresponding to nucleotides 600-1440 of the human MRP3 coding sequence (AF104943) was used to screen a bacteriophage library prepared from mouse testis, and a clone encompassing the entire coding

region was isolated. The cDNA was sequenced and the resulting sequences were assembled using the Sequencher program (Gene Codes Corp., Ann Arbor, MI). The Mrp3 cDNA sequence has been deposited in GenBank (AY841885). A 4.8 kb fragment encompassing the ~ 4.6 kb coding sequence was cloned into the PEAK10 vector (Edge Biosystems, Gaithersburg, MD) to create PEAK10-Mrp3. Human embryonic kidney cells (HEK293/EBNA) were electroporated with 10 μ g of either PEAK10-Mrp3 or the parental plasmid, and individual puromycin-resistant colonies were isolated and expanded for analysis of Mrp3 protein expression. Cells were grown in Dulbecco's modified Eagle's medium supplemented with 10% fetal bovine serum.

Generation of Mrp3 polyclonal antibody and immunoblot analysis. A cDNA fragment encoding amino acids 858-945 of the linker region of Mrp3 was inserted downstream of the glutathione S-transferase coding sequence in the vector pGEX2T, and the induced fusion protein was purified using glutathione Sepharose beads (Amersham Biosciences, Piscataway, NJ). Rabbits were immunized with the recombinant protein, and the immune sera was used for immunoblot analysis. Total cellular lysates prepared from cultured cells, and membrane fractions prepared from liver were subjected to SDS-PAGE and electro-transferred to nitrocellulose filters. Mrp3 antibody was used at a 1:500 dilution and horseradish peroxidase-conjugated secondary antibody (Bio-Rad, NEN, Boston, MA) was used at 1:2,500. Mrp2 monoclonal antibody M2III-5 (kindly provided by George Scheffer, Free University, Amsterdam, The Netherlands) and previously described polyclonal antibody against the bile salt export pump (Wang et al., 2001) were used at 1:1000 dilutions. Affinity purified Mrp4 antisera was raised against amino acids NVDPRTDELIQQKIREK conjugated to KLH (Invitrogen, Carlsbad, CA), and used at a dilution of 1:500. Antibody to β -actin (Sigma-Aldrich, St. Louis, MO) was used at a dilution of 1:1000. Immunoblots were developed using the enhanced chemiluminescence method (Amersham).

Blood Chemistries, Hematology and Histopathology. Animals (mixed 129 x C57BL/6J background from the F3 and F4 generation) were maintained in the Fox Chase laboratory animal facility and housed in a temperature- and humidity-controlled environment under 12-hour light/dark cycles. Mice were fed a standard rodent diet (Lab Diet 5013, PMI Nutrition, Brentwood, MO) and had free access to

water. The Fox Chase Institutional Animal Care and Use Committee approved the protocol. Peripheral blood was obtained by orbital bleeding of anesthetized mice. Blood chemistry and hematology parameters were determined at Antech Diagnostics (Farmingdale, NY). For histological analysis, tissues were fixed in 10% phosphate-buffered formalin, embedded in paraffin, sectioned, and stained with hematoxylin/eosin.

In vivo etoposide toxicity. Groups of male mice (mixed 129 x C57BL/6J background) 8-12 weeks of age were treated with single intraperitoneal injections of etoposide phosphate (Bristol-Myers Squibb, Princeton NJ). Mice were observed daily for a period of 4 weeks. For analysis of white blood cell counts, groups consisting of 5 male mice were treated with a single intraperitoneal injection (150 mg/kg body weight), and blood samples (20 μ l) were taken daily by orbital bleeding for a period of 6 days. White blood cell counts were analyzed using a Coulter Z1 Series Particle Counter (Beckman Coulter, Miami, Florida).

In vitro cytotoxicity assays. Drug sensitivity was analyzed using the CellTiter 96 Cell Proliferation Assay (Promega, Madison WI). Cells seeded overnight in triplicate at ~3,000 cells per well were treated with drugs at various concentrations, and the proliferation assays performed after 72 h of drug exposure. The nonparametric two-tailed Wilcoxon test was used to make inferences about the significance of the data.

Bile duct ligation and analysis of liver and serum bile acids. Mice (mixed 129 x C57BL/6J background) were anesthetized using vaporized isoflurane applied through a nose-cone, and surgery was performed aseptically, using steam-sterilized instruments within a disinfected surgical area. The abdomen was shaved and disinfected with an iodine based surgical scrub and covered with sterile drapes. A 2.0 cm transverse incision was made through the skin of the ventral abdomen at a point starting just below the sternum. A similar incision was made through the body wall. The liver was displaced upwards to expose the bile duct, which was tied off using 6-0 silk, and the body wall closed with interrupted sutures of 6-0 Vicryl. The skin was closed with wound clips, and mice were placed on a warming tray until they recovered from the anesthesia. After 3 days, peripheral blood was sampled from fasting (4 hr) animals, and livers were removed from euthanized animals. Livers were washed in saline, flash-frozen in liquid

nitrogen, and stored at -80°C . Bile acids from pre-weighed, pulverized liver samples were extracted overnight in *tert*-butanol:water (1:1), and liver and serum bile acids were determined using a colorimetric assay (Sigma Diagnostics, St. Louis MO). Serum bilirubin was determined at Antech Diagnostics.

Analysis of bile flow. Bile duct cannulation of mice (mixed 129 x C57BL/6J background) and collection of bile was performed as described previously (Wang et al., 2001). The gall bladder was cannulated after ligation of the common bile duct, and bile was collected at 5 min intervals. At 10 min, taurocholate (100 $\mu\text{m}/\text{kg}$ body weight) was injected as a bolus into the jugular vein. Bile was then collected at 2 min intervals for 10 min, and then at 10 min intervals for 20 min.

Analysis of fecal bile acid excretion, bile acid pool size and composition. Wild-type and *Mrp3*^{-/-} male mice (3-4 months of age; C57BL6/J background) were individually housed in wire bottom cages and stools collected for 3 days. The stools were extracted as described (Turley et al., 1996) and used to determine the total bile acid content by an enzymatic method (Mashige et al., 1981). Pool size was determined as the bile acid content of the small intestine, liver, and gallbladder. These tissues were removed and extracted in ethanol as described (Schwarz et al., 1998). The extract was filtered and bile acid composition was determined using HPLC as described (Torchia et al., 2001). Individual bile acid species were measured using an evaporative light scatter detector (Alltech ELSD 800). Bile acids were identified and quantified by comparison to known amounts of authentic standards purchased from Steraloids (Newport, RI).

Kruskall-Wallis tests, a non-parametric analogue of the Analysis of Variance (ANOVA), were used to compare the distributions of measurements across the four mouse type-treatment combinations. These tests were conducted at a 5% significance level. Next, two-sample Wilcoxon tests were used to make comparisons between all possible pairs of mouse type-treatment combinations. To account for multiple comparisons, Bonferroni adjustment was used to control the experimentwise type I error. Specifically each individual null hypothesis was rejected if the significance level is less than $\alpha = (.05/6) = 0.0083$. These analyses were performed separately for serum conjugated bilirubin, serum bile acids and liver bile acids measurements.

Analysis of Asbt, Ost α , Ost β and Ibabp expression in intestine. RNA was prepared from intestines taken from wild-type and *Mrp3*^{-/-} male mice 3-4 months of age (C57BL6/J background). cDNA synthesis was initiated from 1 μ g of RNA using random hexamer primers and Omniscript transcription reagents (Qiagen). For each real time PCR reaction, cDNA synthesized from 25 ng of RNA was mixed with 2x SYBR Green PCR Master Mix (Applied Biosystems) containing 500 nM of specific primers. The PCR reactions were carried out in triplicate, and samples were analyzed on an ABI 7900 sequence detection system. The oligonucleotide primer sequences were: Asbt, 5'-tgggtttcttctgtagact-3' and 5'-gtttctgcattccagtttcaa-3'; Ost α , 5'-tacaagaacaccctttgccc-3' and 5'-cgaggaatccagagacaaa-3'; Ost β : 5'-gtatttctgtgcagaagatgcg-3' and 5'-tttctgttgccaggatgctc-3'; Ibabp, 5'-caaggctaccgtgaagatgga-3' and 5'-cccacgacctccgaagtct-3'; GAPDH, 5'-tgtgtccgtctggatctga-3' and 5'-cctgettcaccaccttctgat-3'.

Results

Inactivation of the *Mrp3* gene in mice. A targeting construct designed to delete a ~2.1 kb fragment encoding exons 6-8 of the *Mrp3* gene was generated (Fig. 1A). The intended deletion removes 3 exons encoding amino acids 205-332 of the Mrp3 protein, and introduces a frameshift in the reading frame should splicing take place between the exons that immediately border the *neo* marker. The construct was electroporated into R1 embryonic stem cells, and G418/gancyclovir-resistant colonies were isolated. Southern blot analysis of DNA preparations from two ES clones in which proper targeting took place (Fig. 1B) revealed the predicted 5.0 kb (left panel) and 5.7 kb (right panel) bands for the disrupted allele, in addition to the 10.7 kb band for the wild-type allele (left and right panels). Chimeric mice were generated, and germ-line transmission of the disrupted allele was achieved in animals derived from each cell line. Homozygous null mice were identified in litters of backcrossed heterozygote animals (Fig. 1C). Inactivation of the gene was confirmed by immunoblot analysis using polyclonal antisera directed toward Mrp3 protein. Immunoreactive protein of the expected molecular weight was readily detected in crude membranes prepared from liver tissue of wild-type mice, whereas the Mrp3-specific band was absent in

Mrp3^{-/-} mice (Fig. 1D). Haploinsufficiency was apparent in heterozygote mice, in which the level of Mrp3 protein in liver was ~ 50% of that in wild-type mice (Fig. 1D, lane 4).

Heterozygote crosses yielded a distribution of genotypes approximating the expected Mendelian ratios (24.8% wild-type, 49.9% heterozygote, 25.4% null; *n* = 351). *Mrp3*^{-/-} mice were grossly indistinguishable from their wild-type counterparts, had normal viability, and produced litters that were similar in size to those of wild-type mice. The average weight at weaning of male and female *Mrp3*^{-/-} mice was not significantly different from wild-type mice. Histopathological analysis of tissues taken from *Mrp3*^{-/-} mice at 6 weeks and 6 months of age did not reveal obvious abnormalities (data not shown). Serum chemical and hematological parameters measured in ~ 10-week (Table 1) and ~ 9 month old mice did not differ significantly between wild-type and *Mrp3*^{-/-} mice.

Sensitivity of Mrp3-deficient mice to etoposide. The sensitivity of *Mrp3*^{-/-} mice towards anticancer agents was analyzed to ascertain the contribution of the protein to protecting normal tissues. Etoposide was selected as the chemotherapeutic agent in these experiments because human MRP3 is capable of conferring resistance to this compound (Kool et al., 1999; Zelcer et al., 2003; Zeng et al., 1999). Etoposide phosphate, a water-soluble ester of etoposide that is converted to etoposide in plasma, was administered via a single intraperitoneal injection and the sensitivities of wild-type and *Mrp3*^{-/-} mice were compared. Preliminary experiments indicated that the LD50s of wild-type and *Mrp3*^{-/-} mice were similar, and fell between 125 and 250 mg/kg (data not shown). When this dosage range was examined in detail significant differences in the chemosensitivity of wild-type and *Mrp3*^{-/-} mice were not observed (Table 2). The estimated LD50 for both groups of mice was ~ 193 mg/kg body weight.

Damage to hematopoietic tissue is the a toxicity of etoposide. Therefore white blood cell counts were analyzed in the two groups of treated mice. In accord with results described above, the effect of this agent on white blood cell counts of wild-type and *Mrp3*^{-/-} mice were indistinguishable with respect to the time and depth of white blood cell count depression and the time to recovery (Fig. 2).

Analysis of the *in vitro* drug resistance activity of Mrp3. Whereas the drug resistance activity of human MRP3 has been determined, the activity of the rodent pump has not been reported. To confirm

that the results of the chemosensitivity experiments were not attributable to species-specific differences in resistance properties, the Mrp3 cDNA was isolated [Mrp3 protein was 81% identical to human MRP3 (Belinsky et al., 1998) and 92% identical to rat Mrp3 (NM080581)] and expressed in HEK293 cells. HEK-Mrp3-1 and HEK-Mrp3-2, two Mrp3-transfectantants (Fig. 1, panel D, lane 2, and data not shown), exhibited 2.5 and 2.0 fold resistance towards etoposide, respectively, compared to parental vector-transfected cells ($p < .05$; data not shown). This activity was comparable to that of human MRP3 expressed in the same cellular background, for which we previously reported 3-4-fold resistance to this agent (Belinsky et al., 1998).

Analysis of liver function in bile duct-ligated *Mrp3*^{-/-} mice. To determine if Mrp3 is able to protect cholestatic liver by functioning as a basolateral export system for bile acids and other conjugates, the effects of bile duct ligation in wild-type and *Mrp3*^{-/-} mice were analyzed. Bile acids and glucuronides are established substrates of human and rodent Mrp3 (Hirohashi et al., 1999; Hirohashi et al., 2000; Zeng et al., 2000). Therefore, levels of serum bilirubin glucuronide, a compound that is formed in the liver by glucuronidation, and of liver and serum bile acids, were analyzed. The *Mrp3* null mice exhibited abnormalities in each of these parameters that were consistent with the proposed hepatic basolateral export function.

Cholestasis was achieved after 3 days of bile duct ligation, as indicated by marked elevations in liver bile acids in both bile duct-ligated wild-type and *Mrp3* null mice by comparison with their respective sham-ligated controls (Fig. 3A). However, under these conditions, liver bile acid levels in the bile duct-ligated *Mrp3*^{-/-} mice were elevated 1.5 fold by comparison with the bile duct-ligated wild-type mice ($p = 0.0074$). Under non-bile duct ligation (i.e., sham surgery) conditions liver bile acids were also elevated in *Mrp3*^{-/-} mice compared to wild-type mice (Fig. 3A), and serum bile acids were depressed in bile duct-ligated *Mrp3*^{-/-} mice compared to bile duct-ligated control mice (Fig. 3B), but these differences did not reach statistical significance. Serum levels of conjugated bilirubin, which were too low to be measured under non-bile duct ligation conditions, were significantly depressed (~ 67%; $p = 0.0005$) in bile duct-ligated *Mrp3*^{-/-} mice compared to bile duct-ligated wild-type animals (Fig. 3C). Comparable levels of

necrosis, inflammation and portal expansion were observed in the livers of the bile duct-ligated *Mrp3*^{-/-} and corresponding wild-type mice (data not shown).

The effects of bile duct ligation on protein expression levels of Mrp3 (wild-type mice), as well as on expression of other ATP binding cassette transporters whose activities could impact liver parameters, were analyzed (Fig. 4). These pumps included Mrp2 and the bile salt export pump (Bsep), two canalicular transporters that efflux glucuronides and bile acids, respectively, and Mrp4, a sinusoidal pump that transports both of these types of compounds (Chen et al., 2001; Cui et al., 1999; Gerloff et al., 1998; Rius et al., 2003). Mrp3 levels were comparable in the sham and bile duct-ligated wild-type mice. Mrp2 levels were slightly depressed in both wild-type and *Mrp3*^{-/-} bile duct-ligated mice compared to the respective sham-operated control mice, as expected (Paulusma et al., 2000), whereas expression levels of the bile salt export pump and Mrp4 were similar in the four groups of animals. No statistically significant differences were observed when protein levels were quantitated and normalized to the actin control.

Analysis of bile flow in *Mrp3*^{-/-} mice. In view of the abundance of Mrp3 in liver (Fig. 4), measurements were made to determine whether deficiency of Mrp3 affects this bile flow. Differences in bile flow were not detected. Basal bile flow rates were 6.0 ± 1.4 $\mu\text{l}/\text{min}/100\text{g}$ and 6.7 ± 1.5 $\mu\text{l}/\text{min}/100\text{g}$ body weight ($p > 0.4$), and taurocholate-stimulated bile flow rates increased to 13.0 ± 2.5 $\mu\text{l}/\text{min}/100\text{g}$ and 13.1 ± 2.3 $\mu\text{l}/\text{min}/100\text{g}$ body weight ($p > 0.9$), in wild-type and *Mrp3*^{-/-} mice, respectively.

Analysis of bile acid pool size and fecal excretion in *Mrp3*^{-/-} mice. It has been proposed that Mrp3 functions as an intestinal basolateral transporter in the enterohepatic circulation of bile acids. To test that hypothesis, bile acid metabolism was examined in the wild-type and *Mrp3*^{-/-} mice. As shown in Fig. 5A, fecal bile acid secretion was not significantly different in the wild-type and *Mrp3*^{-/-} mice (11.40 ± 2.85 versus 12.96 ± 3.96 ; $p > 0.33$). Further analysis revealed that the bile acid pool size and composition were also similar in wild-type and *Mrp3*^{-/-} mice (Fig. 5B). The mass and percent composition values for all the major bile acid species including taurocholate, tauro- β -muricholate, taurodeoxycholate, tauroursodeoxycholate, and taurochenodeoxycholate, were similar for the two genotypes, with

taurocholate and tauro- β -muricholate accounting for $\sim 80\%$ of the pool. A crude fractional turnover rate can be calculated, because the daily rate of fecal bile acid excretion and bile acid pool size were measured in the same animals. The bile acid fractional turnover rate (daily fecal excretion/pool size) was also similar in the two genotypes (Fig. 5C; wild-type, 0.27 ± 0.09 versus *Mrp3*^{-/-}, 0.33 ± 0.08 ; $p > 0.15$).

Analysis of intestinal bile acid transporter gene expression in *Mrp3*^{-/-} mice. To confirm that the lack of impairment in intestinal bile acid absorption by *Mrp3*^{-/-} mice is not attributable to compensatory alterations in the expression of other intestinal basolateral bile acid transporters, mRNA expression of *Asbt*, which is responsible for uptake of bile acids across the brush border, the recently described *Ost α / β* , which is a candidate basolateral bile acid transporter (Dawson et al., 2004), and *Ibabp* mRNA, an established FXR target gene and an indirect indicator of bile acid flux through the ileum (Chen et al., 2003; Grober et al., 1999), were analyzed in wild-type and *Mrp3*^{-/-} mice. *Asbt*, *Ost α* , *Ost β* , and *Ibabp* mRNA expression did not significantly differ between the wild-type and *Mrp3* null animals (data not shown).

Discussion

In the present study *Mrp3*^{-/-} mice generated by targeted disruption were analyzed in order to determine the *in vivo* functions of the transporter. Although human MRP3 is an established cellular resistance factor for etoposide, our experiments did not reveal enhanced chemosensitivity of *Mrp3*^{-/-} mice. In addition, *Mrp3*^{-/-} mice did not exhibit increased hematopoietic damage, a major toxicity of etoposide. These findings contrast with *Mrp1*^{-/-} mice, which exhibit etoposide sensitivity associated with increased hematopoietic damage (Lorico et al., 1997; Wijnholds et al., 1997). The experiments showing that ectopic expression of *Mrp3* in HEK293 cells is able to confer 2.0-2.5 fold resistance to etoposide, a potency that is only ~ 2 -fold lower than reported for *Mrp1* expressed in HEK293 cells (Stride et al., 1997), indicates that the lack of chemosensitivity is not attributable to the inability of the murine protein to transport etoposide, and instead suggests that the presence of redundant functions masks the contribution of *Mrp3* to protecting normal tissues. A report showing that MRP1 is expressed at higher levels than MRP3 in human

hematopoietic cells suggests that relatively low levels of Mrp3 expression in chemosensitive cells may be an additional factor that bears on the lack of sensitization in *Mrp3*^{-/-} mice (Laupeze et al., 2001). It is worth mentioning that our experiments on the impact of the pump on the *in vivo* chemosensitivity of normal tissues do not preclude the possibility that MRP3 may function as a resistance factor in tumors, a notion that is supported by studies showing that MRP3 is expressed in several cancers and a report in which a correlation between MRP3 expression and clinical outcome was found (e.g., Nies et al., 2001; Steinbach et al., 2003).

A major finding of our study is that Mrp3 functions to protect cholestatic hepatocytes from endobiotics. Serum levels of hepatic constituents such as bile acids and bilirubin glucuronide increase in cholestatic conditions, indicating that hepatocytes are able to deploy basolateral systems to efflux these compounds into sinusoidal blood. Several observations suggested that MRP3 functions as one of these systems. Conjugated bile acids such as glycocholate in the case of human MRP3, and glycocholate and taurocholate in the case of the rat protein, are established substrates of MRP3 (Hirohashi et al., 2000; Zeng et al., 2000), and MRP3 is induced in sinusoidal membranes of hepatocytes in humans with Dubin-Johnson syndrome, a disorder caused by hereditary deficiency of MRP2 and whose principal manifestation is jaundice (Konig et al., 1999). Induction of Mrp3 has also been reported in rats with experimentally induced obstructive jaundice, in *Bsep*^{-/-} mice fed a diet supplemented with cholic acid, and in rat strains that are deficient in Mrp2, the latter of which facilitated isolation of the rat Mrp3 cDNA from liver (Donner and Keppler, 2001; Hirohashi et al., 1998; Soroka et al., 2001; Wang et al., 2003). In addition, induction of MRP3 is mediated by transcriptional pathways associated with bile acids. Bile acids and CAR activators induce expression of Mrp3 *in vivo*, and induction of MRP3 in Caco2 cells was attributed to FTF-like elements in the MRP3 promoter (Inokuchi et al., 2001; Xiong et al., 2002; Zollner et al., 2003). Further, *Tnfr*^{-/-} mice fail to induce Mrp3, and induction is impaired in *Car*^{-/-} mice (Bohan et al., 2003; Zhang et al., 2004). While these observations suggested that MRP3 may be an alternate pathway of bile acid export from hepatocytes, a direct analysis of MRP3 function *in vivo* has not been reported. Here we provide direct evidence that Mrp3 protects cholestatic hepatocytes from bile acids by showing that

Mrp3^{-/-} mice subjected to bile duct ligation have elevated levels of liver bile acids. Moreover, the finding that serum bilirubin levels are elevated in *Mrp3*^{-/-} mice indicates that the protective function of Mrp3 extends to glucuronides as well. These differences in liver parameters were detectable in our experiments after only 3 days of bile duct ligation, a relatively short time frame that was selected so as to minimize the impact of progressive adaptive changes in liver homeostatic mechanisms on the phenotype of *Mrp3*^{-/-} mice. Notably, this short time frame may explain why differences in liver pathology were not observed between wild-type and *Mrp3*^{-/-} mice. In connection with our assessment of Mrp3 function in liver, it should be mentioned that, in the absence of induction, Mrp3 expression in liver is very low or undetectable in rats and humans (Donner and Keppler, 2001; Soroka et al., 2001), whereas in mouse Mrp3 expression is readily detectable in liver (Fig. 3). Hence, our data suggest that Mrp3-mediated protection of cholestatic mouse liver is afforded by the basal levels of murine Mrp3 expression. In addition, it is important to bear in mind that Mrp3 is likely to represent only one of the basolateral membrane systems that are deployed to protect cholestatic hepatocytes. Mrp4 may be another system, as suggested by reports showing that human MRP4 is able to transport glucuronides and bile acids, and that mouse Mrp4 is localized to sinusoidal hepatocyte membranes and induced 7-14 days after bile duct ligation (Chen et al., 2001; Denk et al., 2004; Rius et al., 2003).

In contrast to apical transport across the intestinal apical brush border membrane, there is limited information regarding the mechanisms and transporters responsible for bile acid efflux across the basolateral membrane (Shneider, 2001). Previous *in vitro* studies using rat ileal basolateral membrane vesicles have demonstrated bile acid anion exchange (Weinberg et al., 1986) as well as ATP-dependent bile acid transport activity (Shoji et al., 2004). However, the relative *in vivo* contribution of these transport activities to basolateral bile acid export is unknown. Although Mrp3 was considered to be a candidate for the intestinal basolateral bile acid transporter based on its intestinal expression, localization to the basolateral surface, and ability to transport various bile acid species (Hirohashi et al., 2000; Rost et al., 1999; Scheffer et al., 2002; Zeng et al., 2000), we found that disruption of *Mrp3* did not result in significant changes in intestinal bile acid absorption, as indicated by the lack of significant changes in

fecal bile acid excretion, bile acid pool size, or the calculated fractional turnover rate for bile acids. These results indicate that Mrp3 is not essential for efficient intestinal absorption of bile acids and that additional transporters must be present to mediate basolateral bile acid efflux in ileum and other Asbt-expressing tissues. One such carrier is the recently described Organic Solute Carrier (OST) alpha/beta (OST α/β) (Seward et al., 2003). In the mouse, Ost α/β fulfills many of the criteria for a dedicated basolateral bile acid transporter, including tissue expression that closely parallels that of Asbt, basolateral membrane localization, positive regulation by bile acids, and the ability to efflux all the major species of bile acids (Dawson et al., 2004). While it is possible that Mrp3 functions in conjunction with Ost α/β to mediate intestinal basolateral bile acid transporter, the lack of any compensatory increase in Ost α/β expression suggests that Mrp3 contributes little to the intestinal reclamation of bile acids.

References

- Belinsky MG, Bain LJ, Balsara BB, Testa JR and Kruh GD (1998) Characterization of MOAT-C and MOAT-D, new members of the MRP/cMOAT subfamily of transporter proteins. *J Natl Cancer Inst* **90**:1735-1741.
- Bohan A, Chen WS, Denson LA, Held MA and Boyer JL (2003) Tumor necrosis factor alpha-dependent up-regulation of Lrh-1 and Mrp3(Abcc3) reduces liver injury in obstructive cholestasis. *J Biol Chem* **278**:36688-98.
- Chen F, Ma L, Dawson PA, Sinal CJ, Sehayek E, Gonzalez FJ, Breslow J, Ananthanarayanan M and Shneider BL (2003) Liver receptor homologue-1 mediates species- and cell line-specific bile acid-dependent negative feedback regulation of the apical sodium-dependent bile acid transporter. *J Biol Chem* **278**:19909-16.
- Chen Z-S, Lee K and Kruh GD (2001) Transport of cyclic nucleotides and estradiol 17-b-D-glucuronide by multidrug resistance protein 4. Resistance to 6-mercaptopurine and 6-thioguanine. *J Biol Chem* **276**:33747-54.
- Cui Y, Konig J, Buchholz JK, Spring H, Leier I and Keppler D (1999) Drug resistance and ATP-dependent conjugate transport mediated by the apical multidrug resistance protein, MRP2, permanently expressed in human and canine cells. *Mol Pharmacol* **55**:929-37.
- Dawson PA, Craddock AL, Haywood J, Hubbert M and Ballatori N (2004) The heteromeric organic solute transporter (OST) alpha and beta complex is an ileal basolateral bile acid transporter. *Hepatology* **40**:271A.
- Denk GU, Soroka CJ, Takeyama Y, Chen WS, Schuetz JD and Boyer JL (2004) Multidrug resistance-associated protein 4 is up-regulated in liver but down-regulated in kidney in obstructive cholestasis in the rat. *J Hepatol* **40**:585-91.
- Donner MG and Keppler D (2001) Up-regulation of basolateral multidrug resistance protein 3 (Mrp3) in cholestatic rat liver. *Hepatology* **34**:351-9.

- Gerk PM and Vore M (2002) Regulation of expression of the multidrug resistance-associated protein 2 (MRP2) and its role in drug disposition. *J Pharmacol Exp Ther* **302**:407-15.
- Gerloff T, Stieger B, Hagenbuch B, Madon J, Landmann L, Roth J, Hofmann AF and Meier PJ (1998) The sister of P-glycoprotein represents the canalicular bile salt export pump of mammalian liver. *J Biol Chem* **273**:10046-50.
- Grober J, Zaghini I, Fujii H, Jones SA, Kliewer SA, Willson TM, Ono T and Besnard P (1999) Identification of a bile acid-responsive element in the human ileal bile acid-binding protein gene. Involvement of the farnesoid X receptor/9-cis-retinoic acid receptor heterodimer. *J Biol Chem* **274**:29749-54.
- Hirohashi T, Suzuki H, Ito K, Ogawa K, Kume K, Shimizu T and Sugiyama Y (1998) Hepatic expression of multidrug resistance-associated protein-like proteins maintained in eisai hyperbilirubinemic rats. *Mol Pharmacol* **53**:1068-75.
- Hirohashi T, Suzuki H and Sugiyama Y (1999) Characterization of the transport properties of cloned rat multidrug resistance-associated protein 3 (MRP3). *J Biol Chem* **274**:15181-5.
- Hirohashi T, Suzuki H, Takikawa H and Sugiyama Y (2000) ATP-dependent transport of bile salts by rat multidrug resistance-associated protein 3 (Mrp3). *J Biol Chem* **275**:2905-10.
- Inokuchi A, Hinoshita E, Iwamoto Y, Kohno K, Kuwano M and Uchiumi T (2001) Enhanced expression of the human multidrug resistance protein 3 by bile salt in human enterocytes: A transcriptional control of a plausible bile acid transporter. *J Biol Chem* **276**:46822-46829.
- Johnson DR, Finch RA, Lin ZP, Zeiss CJ and Sartorelli AC (2001) The pharmacological phenotype of combined multidrug-resistance mdr1a/1b- and mrp1-deficient mice. *Cancer Res* **61**:1469-76.
- Konig J, Rost D, Cui Y and Keppler D (1999) Characterization of the human multidrug resistance protein isoform MRP3 localized to the basolateral hepatocyte membrane. *Hepatology* **29**:1156-63.
- Kool M, van der Linden M, de Haas M, Scheffer GL, de Vree JM, Smith AJ, Jansen G, Peters GJ, Ponne N, Scheper RJ, Elferink RP, Baas F and Borst P (1999) MRP3, an organic anion transporter able to transport anti-cancer drugs. *Proc Natl Acad Sci U S A* **96**:6914-9.

- Kruh GD and Belinsky MG (2003) The MRP family of drug efflux pumps. *Oncogene* **22**:7537-52.
- Laupeze B, Amiot L, Payen L, Drenou B, Grosset JM, Lehne G, Fauchet R and Fardel O (2001) Multidrug resistance protein (MRP) activity in normal mature leukocytes and CD34-positive hematopoietic cells from peripheral blood. *Life Sci* **68**:1323-31.
- Lorico A, Rappa G, Finch RA, Yang D, Flavell RA and Sartorelli AC (1997) Disruption of the murine MRP (multidrug resistance protein) gene leads to increased sensitivity to etoposide (VP-16) and increased levels of glutathione. *Cancer Res* **57**:5238-42.
- Mashige F, Tanaka N, Maki A, Kamei S and Yamanaka M (1981) Direct spectrophotometry of total bile acids in serum. *Clin Chem* **27**:1352-6.
- Nies AT, Konig J, Pfannschmidt M, Klar E, Hofmann WJ and Keppler D (2001) Expression of the multidrug resistance proteins MRP2 and MRP3 in human hepatocellular carcinoma. *Int J Cancer* **94**:492-9.
- Paulusma CC, Kothe MJ, Bakker CT, Bosma PJ, van Bokhoven I, van Marle J, Bolder U, Tytgat GN and Oude Elferink RP (2000) Zonal down-regulation and redistribution of the multidrug resistance protein 2 during bile duct ligation in rat liver. *Hepatology* **31**:684-93.
- Rius M, Nies AT, Hummel-Eisenbeiss J, Jedlitschky G and Keppler D (2003) Cotransport of reduced glutathione with bile salts by MRP4 (ABCC4) localized to the basolateral hepatocyte membrane. *Hepatology* **38**:374-84.
- Rost D, Kartenbeck J and Keppler D (1999) Changes in the localization of the rat canalicular conjugate export pump Mrp2 in phalloidin-induced cholestasis. *Hepatology* **29**:814-21.
- Rost D, Mahner S, Sugiyama Y and Stremmel W (2002) Expression and localization of the multidrug resistance-associated protein 3 in rat small and large intestine. *Am J Physiol Gastrointest Liver Physiol* **282**:G720-6.
- Scheffer GL, Kool M, de Haas M, de Vree JM, Pijnenborg AC, Bosman DK, Elferink RP, van der Valk P, Borst P and Scheper RJ (2002) Tissue distribution and induction of human multidrug resistant protein 3. *Lab Invest* **82**:193-201.

- Schultz MJ, Wijnholds J, Peppelenbosch MP, Vervoordeldonk MJ, Speelman P, van Deventer SJ, Borst P and van der Poll T (2001) Mice lacking the multidrug resistance protein 1 are resistant to Streptococcus pneumoniae-induced pneumonia. *J Immunol* **166**:4059-64.
- Schwarz M, Russell DW, Dietschy JM and Turley SD (1998) Marked reduction in bile acid synthesis in cholesterol 7 α -hydroxylase-deficient mice does not lead to diminished tissue cholesterol turnover or to hypercholesterolemia. *J Lipid Res* **39**:1833-43.
- Seward DJ, Koh AS, Boyer JL and Ballatori N (2003) Functional complementation between a novel mammalian polygenic transport complex and an evolutionarily ancient organic solute transporter, OST α -OST β . *J Biol Chem* **278**:27473-82.
- Shneider BL (2001) Intestinal bile acid transport: biology, physiology, and pathophysiology. *J Pediatr Gastroenterol Nutr* **32**:407-17.
- Shoji T, Suzuki H, Kusuhara H, Watanabe Y, Sakamoto S and Sugiyama Y (2004) ATP-dependent transport of organic anions into isolated basolateral membrane vesicles from rat intestine. *Am J Physiol Gastrointest Liver Physiol* **287**:G749-56.
- Soroka CJ, Lee JM, Azzaroli F and Boyer JL (2001) Cellular localization and up-regulation of multidrug resistance-associated protein 3 in hepatocytes and cholangiocytes during obstructive cholestasis in rat liver. *Hepatology* **33**:783-91.
- Steinbach D, Wittig S, Cario G, Viehmann S, Mueller A, Gruhn B, Haefer R, Zintl F and Sauerbrey A (2003) The multidrug resistance-associated protein 3 (MRP3) is associated with a poor outcome in childhood ALL and may account for the worse prognosis in male patients and T-cell immunophenotype. *Blood* **102**:4493-449.
- Stride BD, Grant CE, Loe DW, Hipfner DR, Cole SPC and Deeley RG (1997) Pharmacological characterization of the murine and human orthologs of multidrug-resistance protein in transfected human embryonic kidney cells. *Mol Pharmacol* **52**:344-53.

- Torchia EC, Labonte ED and Agellon LB (2001) Separation and quantitation of bile acids using an isocratic solvent system for high performance liquid chromatography coupled to an evaporative light scattering detector. *Anal Biochem* **298**:293-8.
- Turley SD, Daggy BP and Dietschy JM (1996) Effect of feeding psyllium and cholestyramine in combination on low density lipoprotein metabolism and fecal bile acid excretion in hamsters with dietary-induced hypercholesterolemia. *J Cardiovasc Pharmacol* **27**:71-9.
- Wang R, Lam P, Liu L, Forrest D, Yousef IM, Mignault D, Phillips MJ and Ling V (2003) Severe cholestasis induced by cholic acid feeding in knockout mice of sister of P-glycoprotein. *Hepatology* **38**:1489-99.
- Wang R, Salem M, Yousef IM, Tuchweber B, Lam P, Childs SJ, Helgason CD, Ackerley C, Phillips MJ and Ling V (2001) Targeted inactivation of sister of P-glycoprotein gene (spgp) in mice results in nonprogressive but persistent intrahepatic cholestasis. *Proc Natl Acad Sci U S A* **98**:2011-6.
- Weinberg SL, Burckhardt G and Wilson FA (1986) Taurocholate transport by rat intestinal basolateral membrane vesicles. Evidence for the presence of an anion exchange transport system. *J Clin Invest* **78**:44-50.
- Wijnholds J, Evers R, van Leusden MR, Mol CA, Zaman GJ, Mayer U, Beijnen JH, van der Valk M, Krimpenfort P and Borst P (1997) Increased sensitivity to anticancer drugs and decreased inflammatory response in mice lacking the multidrug resistance-associated protein. *Nat Med* **3**:1275-9.
- Xiong H, Yoshinari K, Brouwer KL and Negishi M (2002) Role of constitutive androstane receptor in the in vivo induction of Mrp3 and CYP2B1/2 by phenobarbital. *Drug Metab Dispos* **30**:918-23.
- Zelcer N, Huisman MT, Reid G, Wielinga P, Breedveld P, Kuil A, Knipscheer P, Schellens JH, Schinkel AH and Borst P (2003) Evidence for two interacting ligand binding sites in human multidrug resistance protein 2 (ATP binding cassette C2). *J Biol Chem* **278**:23538-44.

- Zeng H, Bain LJ, Belinsky MG and Kruh GD (1999) Expression of multidrug resistance protein-3 (multispecific organic anion transporter-D) in human embryonic kidney 293 cells confers resistance to anticancer agents. *Cancer Res* **59**:5964-5967.
- Zeng H, Chen Z-S, Belinsky MG, Rea PA and Kruh GD (2001) Transport of methotrexate (MTX) and folates by multidrug resistance protein (MRP) 3 and MRP1: effect of polyglutamylation on MTX transport. *Cancer Res* **61**:7225-7232.
- Zeng H, Liu G, Rea PA and Kruh GD (2000) Transport of amphipathic anions by human multidrug resistance protein 3. *Cancer Res* **60**:4779-84.
- Zhang J, Huang W, Qatanani M, Evans RM and Moore DD (2004) The Constitutive Androstane Receptor and Pregnane X Receptor Function Coordinately to Prevent Bile Acid-induced Hepatotoxicity. *J Biol Chem* **279**:49517-22.
- Zollner G, Fickert P, Fuchsbichler A, Silbert D, Wagner M, Arbeiter S, Gonzalez FJ, Marschall HU, Zatloukal K, Denk H and Trauner M (2003) Role of nuclear bile acid receptor, FXR, in adaptive ABC transporter regulation by cholic and ursodeoxycholic acid in mouse liver, kidney and intestine. *J Hepatol* **39**:480-8.

Footnotes

This work was supported by the National Institutes of Health grants CA73728 to GDK and DK47987 to PAD, National Cancer Institute Core grant CA06927 to FCCC, and an appropriation from the Commonwealth of Pennsylvania. We thank Andre Rogatko and Eric Ross for assistance with statistical treatment of our data, and Ann L. Craddock and Jamie Haywood for outstanding technical assistance. The current address for Z-S. C. is College of Pharmacy and Allied Health Professions, St. John's University, Jamaica, New York 11439.

Figure Legends

Fig. 1. Targeted disruption of the *Mrp3* gene in mice. A. Schematic showing a portion of the 5' end of the *Mrp3* gene, the targeting construct, the targeted allele, predicted endonuclease restriction products and location of 5' and 3' probes used in southern blot analysis. The *neomycin* cassette is designed to replace three exons of the *Mrp3* locus (corresponding to nucleotides 615-999 of the *Mrp3* coding region). Splicing around these three exons is predicted to result in a frameshift in the coding sequence. Proper integration introduces an XhoI site. The predicted products of XhoI/XmnI digestion in the wild-type and targeted alleles are shown. The construct also contains a thymidine kinase gene cassette used in the positive/negative selection procedure. B. Southern blot analysis of ES cells with 5' (left panel) and 3' (right panel) probes. The expected wild-type and targeted fragments are shown for 2 ES clones in which targeting was successful. C. Three-primer PCR analysis of tail DNA prepared from the progeny of crosses between *Mrp3*^{+/-} mice. A forward primer common to both wild-type and targeted alleles, and reverse primers derived from the targeted portion of the wild-type allele and the 5' region of the *neomycin* cassette were employed. The wild-type allele and targeted allele generate 790 bp and 330 bp products, respectively. D. Immunoblot analysis of Mrp3 in wild-type, heterozygous and *Mrp3*-null mice. Proteins were resolved by sodium dodecyl sulfate-polyacrylamide gel electrophoresis and transferred to nitrocellulose filters. Mrp3 was detected by immunoblotting with anti-Mrp3 polyclonal antibody. Lane 1, HEK293 cells transfected with parental plasmid (HEK-PEAK10-1; 2 µg total protein); lane 2, HEK293 cells transfected with Mrp3-expression vector (HEK-Mrp3-1; 2 µg total protein). Lane 3, 4, and 5: crude membranes (20 µg) prepared from liver tissue of wild-type, *Mrp3*^{+/-}, and *Mrp3*^{-/-} mice, respectively. The Mrp3 band is indicated by the bracket. A non-specific protein band is also present in the liver samples.

Fig. 2. Analysis of white blood cell counts in *Mrp3*^{-/-} and wild-type mice treated with etoposide. *Mrp3*^{-/-} and wild-type mice (n = 5) were treated with a single intraperitoneal injection of 150 mg/kg etoposide phosphate and white blood cell counts were measured daily over the next 6 days. In the

experiment shown one *Mrp3*^{-/-} mouse died day 3 and one wild-type mouse died day 4 post-injection (deaths are indicated by crosses). Closed symbols, *Mrp3*^{-/-} mice, open symbols, wild-type mice.

Fig. 3. Analysis of liver and serum bile acids and serum bilirubin glucuronide in bile duct-ligated wild-type and *Mrp3*^{-/-} mice. Liver and serum bile acid, and serum bilirubin glucuronide levels, were analyzed in wild-type and *Mrp3*^{-/-} male animals after 3 days of bile duct ligation. *A*, total liver bile acids; *B*, serum bile acids; *C*, serum conjugated bilirubin. *; panel *A* $p = 0.0074$; panel *B*, $p = 0.0009$; panel *C*, $p = 0.0005$ for wild-type bile duct-ligated vs. knock-out bile duct-ligated mice, $p = 0.0007$ for wild-type sham vs. wild-type bile duct-ligated mice, $p = 0.0017$ knock-out sham vs. knock-out bile duct-ligated mice. (See Materials and Methods for statistical analyses). In panel *A*, $N = 8-9$ for bile duct-ligated animals and $n = 3$ for sham-ligated animals; in panels *B* and *C*, $N = 12-13$ for bile duct-ligated animals and $N = 6$ for sham-ligated animals. BDL, bile-duct ligated; WT, wild-type mice; KO, *Mrp3*^{-/-} mice.

Fig. 4. Expression of Mrp3, Mrp2, Bsep and Mrp4 in liver of sham or bile duct-ligated wild-type and *Mrp3*^{-/-} mice. Crude membranes (50 μ g) prepared from livers of *Mrp3*^{-/-} or wild-type mice 3 days after sham surgery or bile-duct ligation were resolved by sodium dodecyl sulfate-polyacrylamide gel electrophoresis and transferred to nitrocellulose filters. Mrp3, Mrp2, Bsep and Mrp4 were detected as described under “Materials and Methods”.

Fig. 5. Analysis of bile acid pool size and fecal excretion in *Mrp3*^{-/-} mice. Mean values \pm S.D. are shown. *A*, fecal bile acid excretion was measured in male mice as described under “Materials and Methods” ($n = 10$). *B*, the mass of bile acid in the enterohepatic circulation was determined by extraction, purification, and quantitation using HPLC ($n = 8$). *C*, the bile acid fractional turnover rate was calculated from the data in panels *A* and *B*. Fecal bile acid excretion, total bile acid pool size and bile acid pool composition, and bile acid fractional turnover rate in *Mrp3*^{-/-} mice were not significantly different from wild-type (WT) mice. TBMC, tauro- β -muricholate; TC, taurocholate.

TABLE 1

Chemical and hematological parameters of wild-type and *Mrp3*^{-/-} mice

Blood and serum were analyzed for the indicated parameters. Groups consisted of 3-5 ten-week old mice.

Parameter	Males		Females	
	<i>Mrp3</i> ^{+/+}	<i>Mrp3</i> ^{-/-}	<i>Mrp3</i> ^{+/+}	<i>Mrp3</i> ^{-/-}
hemoglobin (g/dl)	15.5 ± 0.4	17.0 ± 0.6	17.2 ± 1.0	14.6 ± 3.7
hematocrit (%)	49.6 ± 5.2	55.2 ± 3.7	51.6 ± 3.3	46.0 ± 8.0
wbc (thousands/mm ³)	3.3 ± 0.6	5.1 ± 1.5	4.8 ± 1.2	5.0 ± 1.0
rbc (millions/mm ³)	9.1 ± 0.1	10.1 ± 0.8	10.5 ± 0.6	8.9 ± 1.2
glucose (mg/dl)	158 ± 32	181 ± 41	174 ± 13	160 ± 26
urea nitrogen (mg/dl)	26 ± 2	27 ± 2	25 ± 6	27 ± 3
creatinine (mg/dl)	0.2 ± 0.1	0.3 ± 0.2	0.5 ± 0.1	0.3 ± 0.1
total protein (g/dl)	5.8 ± 0.1	5.8 ± 0.3	5.4 ± 0.2	5.9 ± 0.3
albumin (g/dl)	2.6 ± 0.1	3.2 ± 0.3	3.2 ± 0.1	3.4 ± 0.2
bilirubin, total (mg/dl)	0.2 ± 0.1	0.2 ± 0.1	0.3 ± 0.1	0.3 ± 0.1
alkaline phosphatase (u/l)	75 ± 63	132 ± 20	138 ± 10	152 ± 24
alanine aminotransferase (u/l)	37 ± 14	62 ± 49	52 ± 16	33 ± 25
aspartate aminotransferase (u/l)	151 ± 39	229 ± 116	100 ± 45	184 ± 141
cholesterol (mg/dl)	99 ± 12	123 ± 7	80 ± 7	118 ± 7
calcium (mg/dl)	9.4 ± 1.0	9.7 ± 0.6	9.4 ± 0.3	9.7 ± 0.4
phosphorus (mg/dl)	7.7 ± 2.1	8.9 ± 2.6	7.3 ± 0.9	7.8 ± 1.4
sodium (mEq/l)	160 ± 5	156 ± 5	148 ± 1	157 ± 7
potassium (mEq/l)	7.7 ± 0.7	7.8 ± 1.2	6.8 ± 0.2	7.8 ± 1.3
chloride (mEq/l)	98 ± 16	99 ± 13	87 ± 5	93 ± 10
globulin (g/dl)	3.2 ± 0.4	2.6 ± 0.2	2.3 ± 0.2	2.5 ± 0.1

TABLE 2

Toxicity of etoposide phosphate in wild-type and *Mrp3*-deficient mice

Groups of male mice (age 8-12 weeks) were treated with varying amounts of etoposide phosphate administered as a single intraperitoneal injection. Dosage values are milligrams etoposide phosphate per kilogram body weight. The values represent number of surviving animals per group 4 weeks after treatment.

Dose (mg/kg)	Survival	
	<i>Mrp3</i> ^{+/+}	<i>Mrp3</i> ^{-/-}
125	6/6	6/6
150	13/13	11/13
175	10/14	11/14
200	7/18	7/18
225	6/17	4/17
250	0/5	0/5

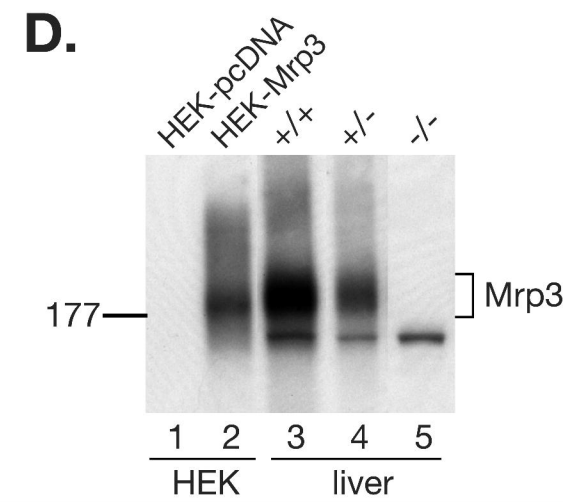
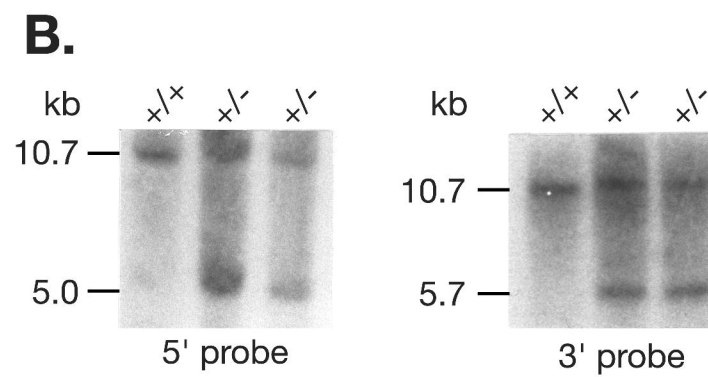
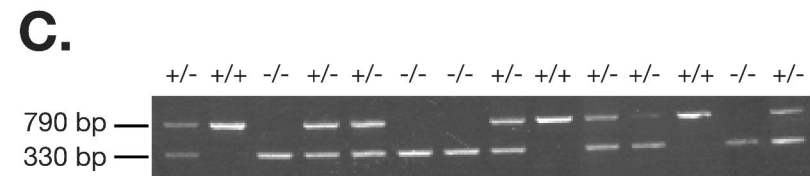
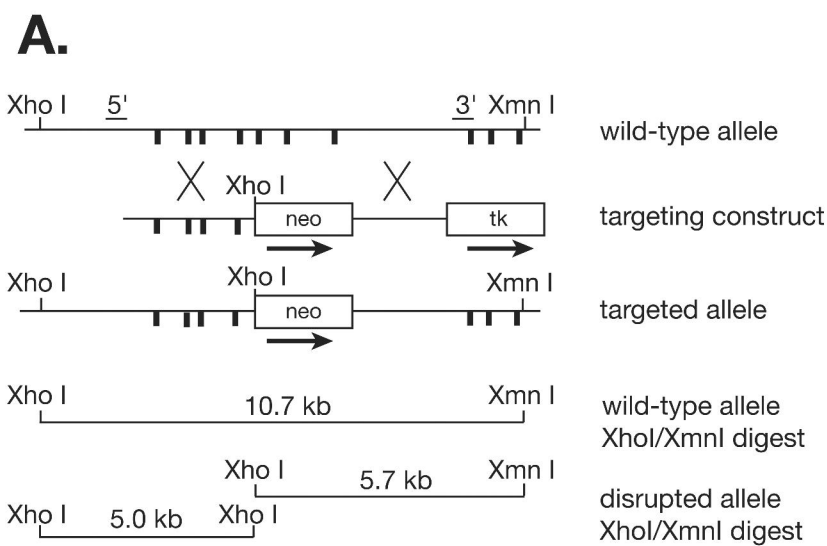


Figure 1

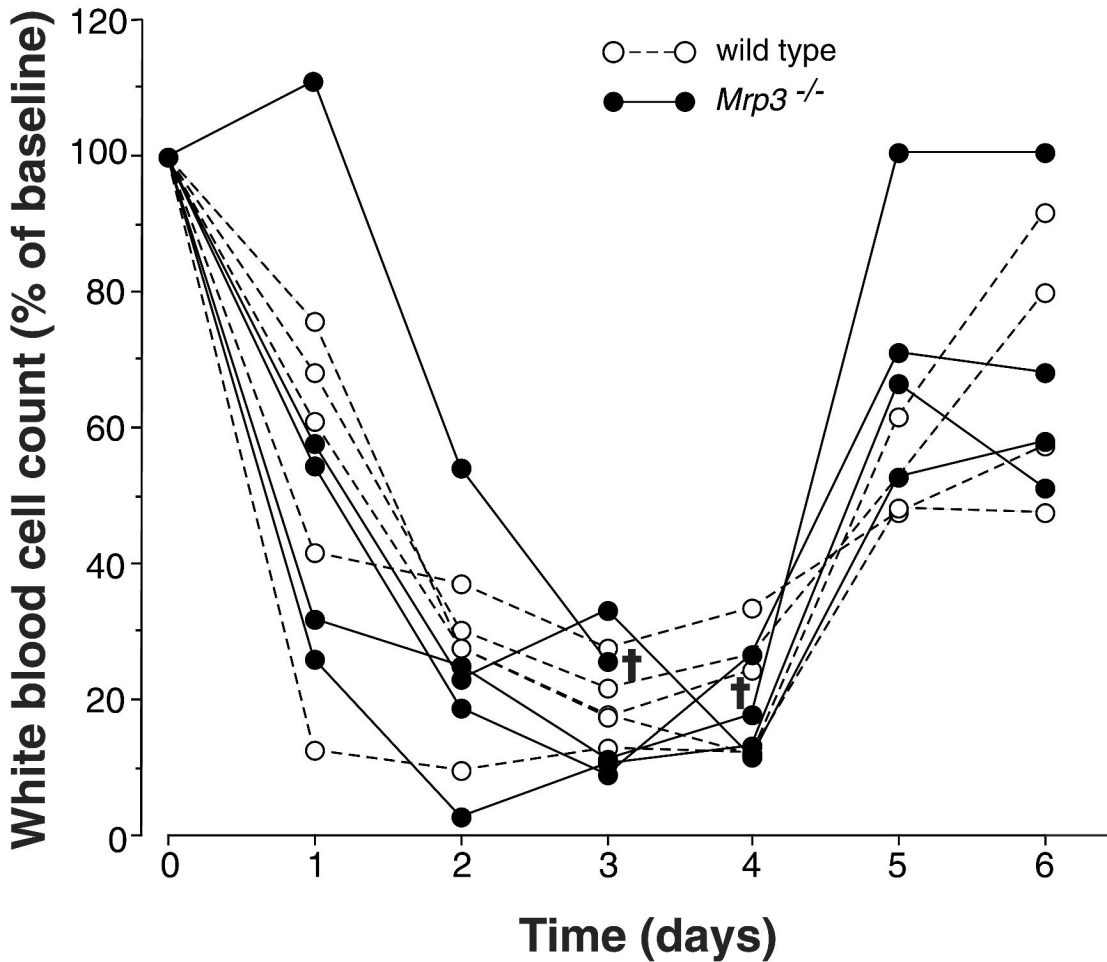


Figure 2

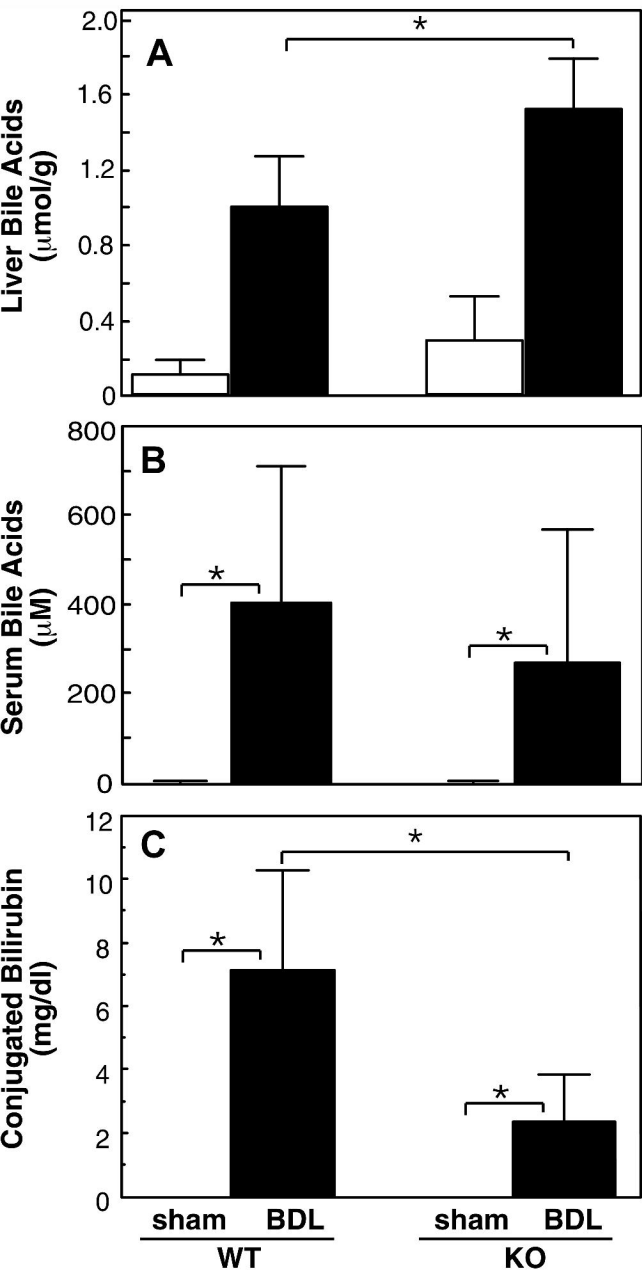


Figure 3

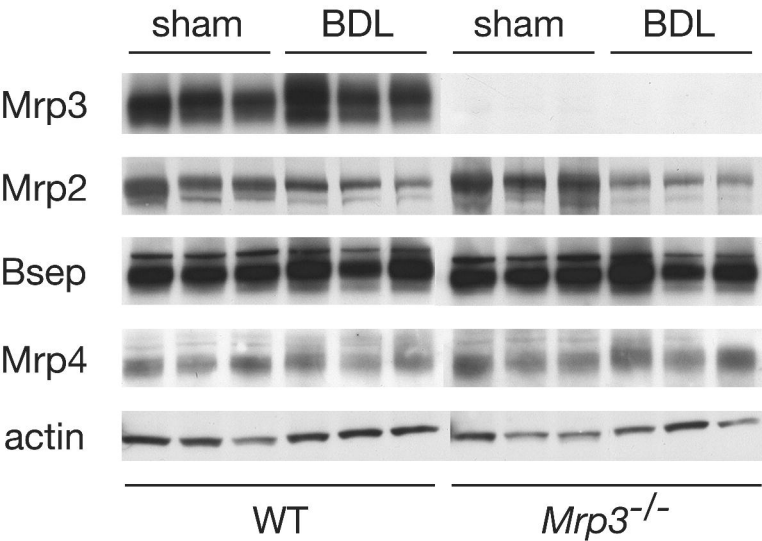


Figure 4

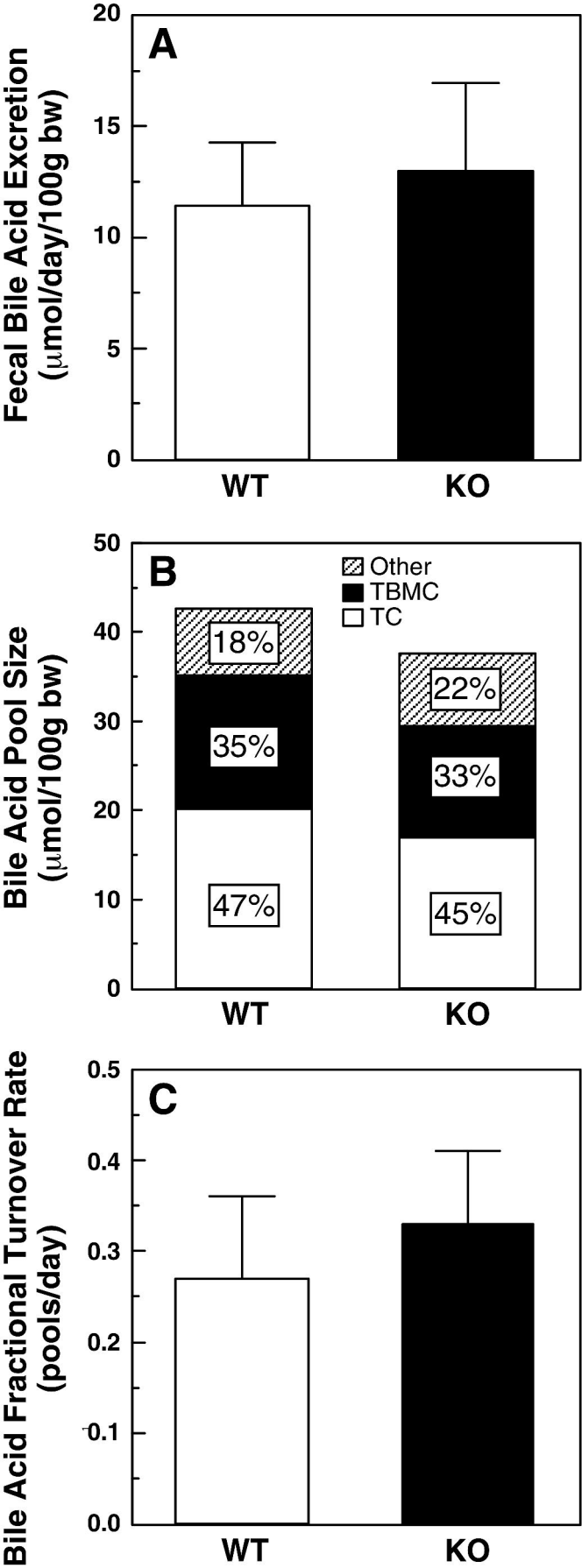


Figure 5